

Tricritical Behavior in the Laser with a Saturable Absorber

Mansour Mortazavi and Surendra Singh

Department of Physics, University of Arkansas, Fayetteville, Arkansas 72701

(Received 10 May 1989)

Nonequilibrium continuous and discontinuous phase transitions in the laser with a saturable absorber have been observed. A novel feature of these measurements is the observation of the tricritical behavior. The adequacy of the perturbative approach to describe saturation effects is discussed in light of these measurements.

PACS numbers: 42.50.-p, 05.70.Ln, 42.55.Bi

Although the lasers with intracavity saturable absorbers (LSA) have been used for a long time in frequency stabilization and Q -switching schemes, their fluctuation properties¹ have received much less experimental attention.² It is known that the laser with a saturable absorber provides several outstanding examples of non-equilibrium phase transitions.^{1,3-6} Depending on its operating parameters the LSA is capable of exhibiting both continuous (second-order) and discontinuous (first-order) phase transitions. In this paper we wish to describe a laser with an intracavity saturable absorber where this discontinuous phase transition has been observed. A novel feature of these measurements is the observation of the associated tricritical point behavior. A tricritical point^{7,8} is the terminus of a line of first-order phase transitions in the parameter space. It is also the junction of a line of first-order phase transitions and a line of second-order phase transitions.

The experimental setup consists of a 40-cm-long optical cavity containing two gas discharge cells with Brewster windows and operating at 632.8 nm. The gain cell is a 10-cm-long cold-cathode discharge tube with a 1-mm bore containing a 7:1 mixture of ^4He : ^{20}Ne at a total gas pressure of 3.5 Torr. The hot-cathode absorber cell is 20 cm long with a 2-mm bore and contains pure ^{20}Ne at a pressure of 0.3 Torr. The discharge current in the absorber tube could be varied from 10 to 30 mA. The output mirror with 0.3% transmissivity was mounted on a piezoelectric transducer (PZT) that allowed the cavity mode frequency to be adjusted relative to the center frequencies of the atomic gain and absorption profiles. With the cavity frequency tuned close to the center of atomic lines the laser operated in a single longitudinal and single transverse mode.

Under the condition of fixed relative detuning between the cavity mode and the atomic gain and absorption profiles, the equation of motion for the dimensionless slowly varying complex field amplitude E of the laser is⁹

$$\dot{E} = E(a + b|E|^2 - |E|^4) + q(t), \quad (1)$$

where $q(t)$ represents spontaneous-emission noise. The dimensionless parameters a and b are related to the gain

and absorption per pass A and \bar{A} and the losses per pass C by

$$\begin{aligned} a &= a'(1 - \bar{A}/A - C/A)n_s^{2/3}, \\ b &= b'(s\bar{A}/A - 1)n_s^{1/3}. \end{aligned} \quad (2)$$

The coefficients a' and b' vary little in the region of interest. For the laser used here they are approximately $\frac{1}{2}$ and $\frac{1}{4}$, respectively. The saturation photon number n_s for the atoms in the gain cell is of the order of 10^8 for our laser. The Doppler linewidth for both the gain and absorber atoms is about 1.5 GHz and pressure-broadened homogeneous linewidths are 270 and 30 MHz, respectively, for the gain and absorber atoms. The ratio s of the saturation photon numbers for the atoms in the gain and absorption cells is determined by pressure broadening and is 9 for our case. A and \bar{A} are proportional to the discharge currents in the two cells. This means that the parameters a and b can be varied independently by varying the discharge currents in the two cells and/or losses in the cavity.

Equation (1) can be converted into a Fokker-Planck equation for the probability density $\mathcal{P}(E)$ of the complex field amplitude. The steady-state solution $\mathcal{P}_s(E)$ of this equation reads⁹

$$\mathcal{P}_s(E) = \text{const} \times e^{-U(E)}, \quad (3)$$

$$U(E) = -\frac{1}{2}a|E|^2 - \frac{1}{4}b|E|^4 + \frac{1}{6}|E|^6.$$

This distribution may exhibit one or two peaks⁹ depending on the values of a and b . These peaks correspond to highly probable states of the laser. For positive values of b this distribution has a single peak corresponding to zero-field amplitude ($r = |E|$, $r^2 = |E|^2 = I$) at $r=0$ in the range $-\infty < a < -b^2/4$. In the range $-b^2/4 < a < 0$, the LSA exhibits bistability and the distribution has two peaks corresponding to zero and nonzero field amplitudes $r=0$ and $r=r_+$, with $r_+^2 = [1 + (1 + 4a/b^2)^{1/2}]b/2$. For negative values of b the probability distribution has only a single peak which is located at $r=0$ for $a < 0$ and at $r=r_+$ with $r_+^2 = [-1 + (1 + 4a/b^2)^{1/2}]|b|/2$ for $a > 0$. The maxi-

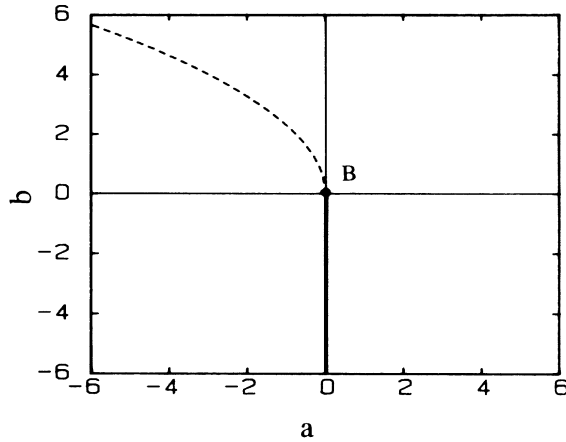


FIG. 1. Phase diagram for the laser with a saturable absorber. The dashed line is the line of first-order phase transitions and the thick line is the line of critical points. Point *B* is the tricritical point.

imum value of the distribution corresponds to the most probable value r_m of the field amplitude. If r_m is treated as the order parameter (analog of magnetization) and $-a$ as the analog of the "temperature" of a system in thermodynamic equilibrium, the LSA exhibits the analogs of discontinuous (first-order) and continuous (second-order) phase transitions in a ferromagnet. The phase diagram for the LSA is shown in Fig. 1. The dashed line $a = -3b^2/16$ is the first-order coexistence curve and the thick line $a = 0$ with $b < 0$ is the line of (second-order) critical points. For a fixed positive value of b , the order parameter r_m changes discontinuously from $r_m = 0$ to $r_m = r_+$ at $a = -3b^2/16$. The behavior of r_m^2 as a function of a for $b = 2$ is shown by the dashed curve in Fig. 2(a). The discontinuity in r_m decreases as b decreases until at $b = 0$ it vanishes and the order parameter changes continuously from $r_m = 0$ to $r_m = |a|^{1/4}$ at $a = 0$. Point *B* ($a = 0 = b$) is an example of a tricritical point where the first-order line meets the line of critical points.⁷ For $b < 0$ the LSA undergoes a second-order phase transition where the order parameter changes smoothly from $r_m = 0$ to $r_m^2 = [-1 + (1 + 4a/b^2)^{1/2}] |b|/2$ at $a = 0$. The dashed curve in Fig. 2(b) shows the variation of r_m^2 for the tricritical case. Figure 2(c) shows the same behavior for the ordinary laser. Note that for the ordinary laser $b = -1$ and the sixth-order term in Eq. (3) is absent.

The stability requirements on the LSA are at least 1 order of magnitude more stringent than those on the conventional laser. This is because in the ordinary laser the parameter $a \sim (1 - C/A)n_s^{1/2} \approx (1 - C/A) \times 10^4$, whereas in the LSA

$$a \sim (1 - \bar{A}/A - C/A)n_s^{2/3} \approx (1 - \bar{A}/A - C/A)2 \times 10^5$$

and this means that the LSA is 10 times more sensitive to any variation of gain and loss. Similarly, the mode

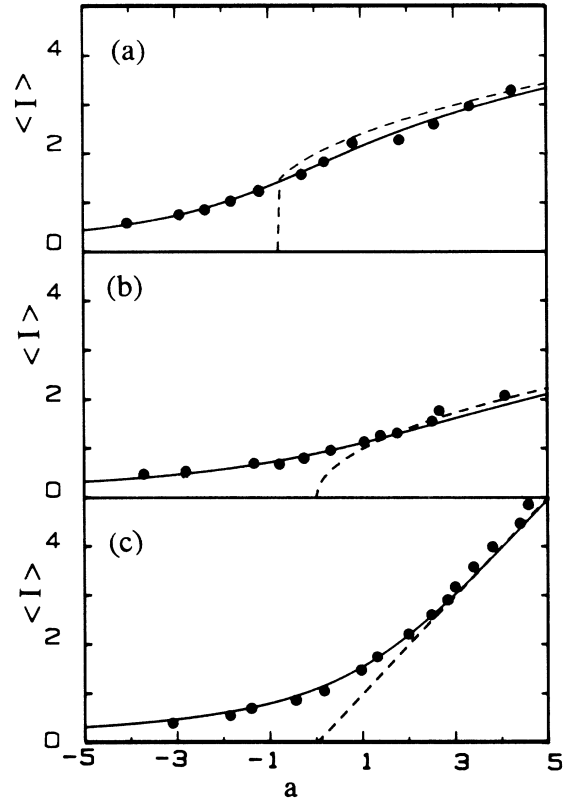


FIG. 2. Measured dimensionless mean light intensity compared with the square of the order parameter (dashed curve) for (a) $b = 2$, corresponding to a discontinuous first-order phase transition, (b) $b = 0$, corresponding to the tricritical behavior, and (c) with the absorber tube turned off. Case (c) corresponds to the ordinary-laser threshold (second-order) transition. The solid curve is the mean intensity calculated from Eq. (3).

frequency must be kept fixed relative to the centers of the atomic gain and absorption profiles. The effect of any frequency drift on A and \bar{A} is very different. Coefficient \bar{A} is a very sensitive function of detuning because of the narrow natural linewidth (about 30 MHz) of atoms in the absorber cell. In view of these requirements the laser cavity was constructed from Invar and aluminum to compensate for temperature expansion. The whole laser assembly was enclosed in a temperature-controlled oven of large heat capacity. Once thermal equilibrium is reached, the laser frequency drifts no more than 5 MHz over a period of 5 min. This was determined by turning the absorber tube off and watching the laser intensity drift with detuning. It was assumed that the same stability was achieved with the absorber tube on. Another problem that one has to contend with is the plasma discharge noise. This was estimated¹⁰ to be less than 0.05 of the intrinsic noise.

Independent variation of the parameters a and b was achieved by keeping the pumping in the gain cell fixed.

The parameter b could then be varied by changing the absorption-cell current and for a fixed absorber-cell current the parameter a could be varied by changing the position of a movable knife edge that partially obstructed the laser beam inside the cavity. Slow drifts of laser light intensity were corrected by means of a feedback amplifier with a time constant of several seconds. This long time constant was chosen to ensure that the feedback electronics do not interfere with the free evolution of the laser. This was found to be satisfactory for all operating regimes reported here.

The main beam was allowed to fall on a 500-kHz photodetector-amplifier combination whose output was proportional to the incident light intensity. The linearity was checked by using a stabilized broadband thermal light source. The detector output was sampled for 100 ns at regular intervals separated by 60 μ s. The sampled values are transferred to the appropriate bins of a multichannel analyzer and a histogram of laser light intensity is built up. For each value of absorber current, measurements for several different working points of the laser were made by varying the losses. Each measurement took 10 s and consisted of 10^5 samples. From the measured histograms mean light intensity $\langle I \rangle$ in units of channel number and its relative variance $\kappa_2 = \langle (I - \langle I \rangle)^2 \rangle / \langle I \rangle^2$, which is independent of units chosen for I , were calculated. The procedure for determining a and b is similar to that used in Ref. 10. The scale factor that relates channel number to light intensity was obtained from the κ_2 vs $\log_{10} \langle I \rangle$ curve. This scale factor corresponds to a translation along the \log_{10} axis. The parameter b was then estimated by plotting the measured relative variance κ_2 against $\log_{10} \langle I \rangle$ and comparing with theoretically computed curves derived from Eq. (3). A single value of b fits the κ_2 vs $\log_{10} \langle I \rangle$ curve quite well for a fixed current in the absorber cell. This means that the variation of a' and b' was small over the range of operating points reported here. For fixed values of A and \bar{A} (fixed amplifying and absorbing currents) the relative change $|\Delta C|/C_0$ in C needed to vary a from -5 to $+5$ is, from Eq. (2),

$$|\Delta C|/C_0 = [|\Delta a|/a'(1 - \bar{A}/A)] n_s^{-2/3} \approx 10^{-4}.$$

Here $C_0 = 1 - \bar{A}/A$ is the value of C for $a = 0$. For this change in C both a' and b' can be treated as constants. Once b was known the pump parameter a was determined from the knowledge of κ_2 . This procedure was found satisfactory except for very low intensities $a < -5$, where electronic noise begins to introduce large uncertainties.¹¹ Test runs with a thermal light source indicated that over the intensity range reported (about a decade) about 90% of the counts fell in two channels. With the laser on, the counts were spread over more than 75 channels.

The results of the experiment are shown in Fig. 2. In lasers the order parameter r_m is not directly observable.

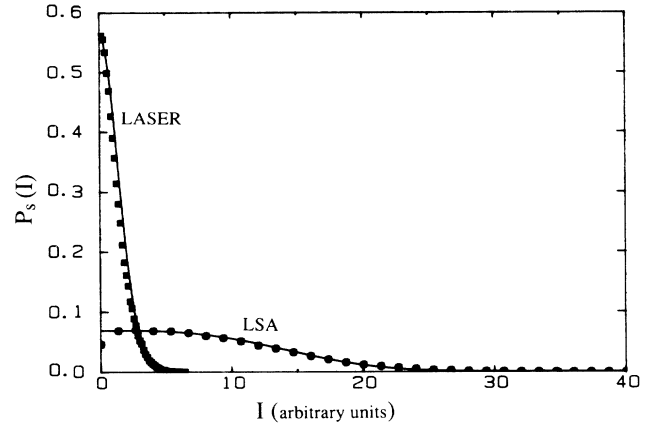


FIG. 3. A comparison of the laser intensity distribution at the tricritical point and at the ordinary-laser threshold. The points are experimental results and the curves are theoretical predictions. In order to facilitate a direct comparison between the two cases we have chosen the intensity scale factor for the LSA to be the same as that for the ordinary laser and the probability density for the LSA has been appropriately scaled.

From the data it was not possible to extract the most probable intensity with good accuracy. This is especially the case in the region where one expects flat distributions. An example is shown in Fig. 3. For this reason we focused on the mean light intensity which can be determined with greater reliability. Mean light intensity has different meaning in different regimes. Above threshold, relative amplitude fluctuations decrease rapidly as a is increased. Therefore, above threshold, the average intensity is just the square of the order parameter r_m except in the immediate neighborhood of threshold. Below threshold the mean light intensity represents the mean-square fluctuations of the field amplitude and is analogous to the mean-square fluctuation of the magnetization. The mean intensity therefore behaves as the zero-field susceptibility of a ferromagnet.

Figure 2(a) shows the behavior of mean light intensity for $b = 2$ where the LSA is expected to undergo a first-order phase transition. Above threshold the mean light intensity quickly follows the predicted behavior of r_m^2 (dashed curve). The change in the curvature of $\langle I \rangle$ vs a in passing the threshold is clearly visible. This change in curvature and steplike behavior becomes more pronounced as we move away from the tricritical point.¹¹ For large values of a we expect $r_m^2 \sim a^{1/2}$. As b is decreased this discontinuous transition changes into a continuous transition at $b = 0$ as shown in Fig. 2(b). The dashed curve is $r_m^2 = |a|^{2\beta_t}$ with tricritical exponent $\beta_t = \frac{1}{4}$. Once again, except for the region near threshold, this dependence is well confirmed. Figure 2(c) shows the behavior of mean light intensity when the absorber tube is turned off. In this case the dashed line represents $r_m^2 = r_m^2 = |a|^{2\beta}$ with the critical exponent $\beta = \frac{1}{2}$ and this

is the dependence expected for the ordinary laser which undergoes a second-order phase transition.¹² In all cases the mean-field phase transitions seem to describe the changes that laser fluctuations undergo in the LSA very well. The rounding effect near threshold is due to the finite size of the laser. It is well known that fluctuations cause deviations from the predictions of mean-field theory. The behavior of the mean light intensity below threshold is analogous to the behavior of the zero-field susceptibility of a ferromagnet. Measurements of zero-field susceptibility are difficult to make in systems in thermodynamic equilibrium because the region of large fluctuations is not easily accessible. The dependence of $\langle I \rangle$ on a away from threshold in each case can be described by $\langle I \rangle \sim |a|^{-\gamma}$ with mean-field exponent $\gamma=1$.

The tricritical behavior observed here is also interesting from the point of view of the theory of oscillators. The LSA with $b=0$ provides a physical example of a sextic oscillator. At the tricritical point the effects of quantum fluctuations are expected to be enhanced compared to the ordinary-laser threshold. This enhancement is clearly reflected in the increased width of the light intensity ($I = |E|^2$) distribution $P_s(I)$ in Fig. 3, where the behavior of this distribution at the tricritical point and at the ordinary-laser threshold is compared. The tricritical behavior in simple terms means that in the region under investigation laser power does not increase linearly with net gain as is the case for the ordinary laser; rather it increases as the square root of the net gain. The tricritical behavior in the LSA has also received a great deal of attention from another point of view. Since quantum fluctuations are amplified near the tricritical point, they may render the fifth-order treatment of saturation effects in the LSA inadequate.¹³ The differences that arise when a more exact theory of saturation effects is used have been carefully investigated by Englund.¹ In the present experiments with $n_s \sim 10^8$ and $\bar{n}_s \approx 10^7$ we find that, at least in the region of threshold, a fifth-order treatment is adequate. This is also confirmed by a detailed analysis of higher-order statistics measured in the experiment.¹¹

The LSA is one of the few nonequilibrium systems that exhibit a sequence of phase transitions both continuous and discontinuous and is rather unique in that it exhibits the tricritical behavior that is accessible to experi-

mental measurements.

This work was supported by the National Science Foundation.

¹J. C. Englund, Ph.D. thesis, University of Texas at Austin, 1985 (unpublished); J. C. Englund and W. C. Schieve, in *Coherence and Quantum Optics V*, edited by L. Mandel and E. Wolf (Plenum, New York, 1984). The first reference is a comprehensive study of fluctuations in the LSA and the dye lasers and provides an extensive list of references in this field. P. Mandel, *Phys. Rev. A* **21**, 2020 (1980). Recent work on the LSA has been summarized by N. B. Abraham, P. Mandel, and L. M. Narducci, in *Progress in Optics*, edited by E. Wolf (North-Holland, Amsterdam, 1988), Vol. XXV.

²S. Ruschin and S. H. Bauer, *Chem. Phys. Lett.* **66**, 100 (1979); E. Arimondo, D. Dangoisse, and L. Fronzoni, *Europhys. Lett.* **4**, 287 (1987); E. Arimondo, D. Dangoisse, C. Gabbanini, E. Menchi, and F. Pappoff, *J. Opt. Soc. Am. B* **4**, 892 (1987).

³J. W. F. Woo and R. Landauer, *IEEE J. Quantum Electron.* **7**, 435 (1971).

⁴J. F. Scott, M. Sargent, III, and C. D. Cantrell, *Opt. Commun.* **15**, 13 (1975).

⁵S. T. Dembinski and A. Kossakowski, *Z. Phys. B* **25**, 207 (1976).

⁶P. H. Lee, P. B. Schoeffler, and W. B. Barker, *Appl. Phys. Lett.* **13**, 373 (1968); V. N. Lisitsyn and V. P. Chebotaev, *Pis'ma Zh. Eksp. Teor. Fiz.* **7**, 3 (1968) [*JETP Lett.* **7**, 1 (1968)].

⁷R. B. Griffiths, *Phys. Rev. B* **7**, 545 (1973).

⁸D. Walgraef, P. Borckmans, and G. Dewel, *Z. Phys. B* **30**, 437 (1978); J. C. Antoranz and M. G. Velarde, *Opt. Commun.* **38**, 61 (1981).

⁹A. P. Kazantsev and G. I. Surdutovich, *Zh. Eksp. Teor. Fiz.* **58**, 245 (1970) [*Sov. Phys. JETP* **31**, 133 (1970)]; A. P. Kazantsev, S. G. Rautian, and G. I. Surdutovich, *Zh. Eksp. Teor. Fiz.* **54**, 245 (1970) [*Sov. Phys. JETP* **27**, 756 (1968)]; H. Greenstein, *J. Appl. Phys.* **43**, 1732 (1972); Mansour Mortazavi and S. Singh, *Phys. Rev. A* **35**, 429 (1987).

¹⁰M. R. Young and S. Singh, *Phys. Rev. A* **38**, 238 (1988).

¹¹Mansour Mortazavi and S. Singh (to be published).

¹²M. Corti and V. Degiorgio, *Phys. Rev. Lett.* **36**, 1173 (1976).

¹³S. T. Dembinski, A. Kossakowski, L. Wolniewicz, L. A. Lugiato, and P. Mandel, *Z. Phys. B* **32**, 107 (1978).